Nanocomposites of Poly(trimethylene terephthalate) with Organoclay

Cheng-Fang Ou

Department of Chemical Engineering, National Chin-Yi Institute of Technology, Taichung 411, Taiwan, Republic of China

Received 22 July 2002; accepted 15 December 2002

ABSTRACT: Two different kinds of clay were organomodified with cetylpyridinium chloride (CPC) as an intercalation agent. Poly(trimethylene terephthalate) (PTT)/organoclay nanocomposites were prepared by the solution intercalation method. Wide-angle X-ray diffraction (WAXD) indicated that the layers of clay were intercalated by CPC and the interlayer spacing was a function of the cationic exchange capacity (CEC) of the clay: the higher the CEC, the larger the interlayer spacing is. The WAXD studies showed that the interlayer spacing of organoclay in the nanocomposites depends on the amount of organoclay. From the results of differential scanning calorimetry analysis it was found that clay behaves as a nucleating agent and enhances the crystallization rate of PTT. The maximum enhancement of the crystallization rate for the nanocomposites was observed in nanocomposites containing about 5 wt % organoclay with a range of 1–15 wt %. The thermal stability of the nanocomposites was enhanced by the addition of 1–10 wt % organoclay as found from thermogravimetric analysis. The thermal stability of the PTT/organoclay nanocomposites was related to the organoclay content and the dispersion in the PTT matrix. © 2003 Wiley Periodicals, Inc. J Appl Polym Sci 89: 3315–3322, 2003

Key words: nanocomposites; clay; crystallization; montmorillonite; intercalation

INTRODUCTION

One of the most prevalent classes of composites is composed of materials containing an organic binding matrix with an inorganic material as the reinforcing filler. Organic/inorganic composites also comprise one of the most important classes of synthetic engineering materials.[1–3] The incorporation of organic/inorganic hybrids can result in materials that possess high degrees of stiffness and strength and gas barrier properties with far less inorganic content than is used in conventionally filled polymer composites. Layered silicates dispersed as a reinforcing phase in an engineering polymer matrix are among the most important forms of such nanocomposites. Clays are usually used as additives.[4–10]

The structure of the composite depends on the extent of compatibility of the organic and inorganic components.[3] However, the lack of affinity between a hydrophilic silicate and hydrophobic polymer makes it difficult to achieve a homogeneous mixture. Compatibility between the silicate clay layer and the polymers is therefore achieved by ion exchange reactions. The hydrated cations of the interlayer can be exchanged with cationic surfactants such alkylammonium. Because the organoclay (or modified clay) is organophilic, its surface energy is lowered and it is more compatible with an organic polymer.[3] These polymers may be able to intercalate within the galleries under well-defined experimental conditions. These polymer-layered silicate nanocomposites can exhibit increased modulus,[5–7] decreased thermal expansion coefficients,[6] reduced gas permeability,[6,8] and increased solvent resistance,[9] when compared to the polymer alone. Several methods of making polymer clay nanocomposites have been demonstrated, including solution mixing, melting, and *in situ* polymerization.[10,11]

Research on polyester/clay nanocomposites is at an early stage, and no products have entered the market as yet. There are some reports in the literature of the preparation of poly(ethylene terephthalate) (PET) nanocomposites.[12,13] Ke et al.[12] have reported the preparation of a PET/clay nanocomposite that had a threefold greater crystallization rate than that of neat PET and showed a heat deflection temperature that was 20–50°C higher than the neat PET. The melting and crystallization behavior of polymers can be investigated using differential scanning calorimetry (DSC). Di Lorenzo et al.[14] have reported on the melting and crystallization behavior of poly(3-hydroxybutyrate) (P3HB) that can be properly modified by copolymerization or blending. Copolymerization of 3HB with another hydroxyalkanoate monomer results in a material with a lower melting temperature. The crystal-

Correspondence to: C.-F. Ou (oucf@chinyi.ncit.edu.tw).
Contract grant sponsor: National Science Council, Republic of China; contract grant number: NSC90-2216-E-167-002.

lization process of P3HB and its copolymers is greatly influenced by the presence of another component for both miscible and immiscible blends. Poly(trimethylene terephthalate) (PTT) is a semicrystalline, polymeric material that is currently being developed by Shell Chemical Company for fiber and engineering thermoplastic applications. In recent years, PTTs have drawn attention for application in the textile industry because of a great reduction in the manufacturing cost of 1,3-propanediol, the monomer used for PTT synthesis.[15] Many studies on PTT have been published.[15–18] To the best of our knowledge, there are very few reports of PTT/organoclay nanocomposite formation by solution blending.

The objectives of this study were to disperse organoclay into a PTT matrix and to investigate the effect of organoclay loadings on the crystallization behaviors and thermal stabilities of PTT/organoclay nanocomposites. An intercalation agent was used to chemically modify the surface of the pristine clay. We also examined the effect of the cationic exchange capacity (CEC) of the clay on the interlayer spacing. These results were analyzed by wide-angle X-ray diffraction (WAXD), DSC, and thermogravimetric analysis (TGA).

EXPERIMENTAL

Materials

Two kinds of sodium montmorillonite (MMT) with CEC values of 87 and 114 meq/100 g (termed 8K and 11K) were provided by Pai-Kong Nano Technology Co. Ltd. (Taoyuan, Taiwan). The PTT resin was kindly donated by Shin Koung Textile Co. (Taoyuan, Taiwan). The resin has an intrinsic viscosity of 0.794 dL/g in 60/40 (w/w) phenol/tetrachloroethane at 30°C. Cetylpyridinium chloride (CPC) was purchased from Tokyo Chemicals Industry. Other materials were commercially available and used as received.

Preparation of organoclay and PTT/organoclay nanocomposites

Five grams of refined clay was added to 200 mL of distilled water. The dispersion was heated to 60°C with mechanical stirring for 1.5 h. The optimum weight of CPC (CPC/clay = 2/1 equivalent weight) was added to the dispersion, and the resultant mixture was stirred at 60°C for 24 h. The solution was filtered, and the organoclay was thoroughly washed 3 times with 1/9 (w/w) alcohol/H_2O and distilled water to remove the residual salt. The organoclays were then dried overnight in a vacuum oven at 70°C, and organoclays termed 8K-P and 11K-P were produced.

Nanocomposites were prepared by solution mixing appropriate quantities of finely ground organoclay 11K-P and PTT in the 3/1 (w/w) phenol/chloroform mixed solvent at 60°C for 2 h. Four nanocomposites with organoclay contents of 1, 5, 10, and 15 wt % were prepared for this study. The resulting nanocomposites were dried in a vacuum at 80°C for 24 h to remove any remaining solvent.

WAXD experiments

The WAXD experiments were performed on powder specimens using a Shimadzu XD-5 diffractometer with Cu Kα radiation (λ = 0.154056 nm). The generator was operated at 300 kV and 20 mA. Samples were scanned from 2θ = 2.0–15.0° at a scanning rate of 2°/min.

DSC measurements

DSC was employed to characterize the crystallization and thermal behaviors of the nanocomposites. A TA 2010 system was used under a nitrogen atmosphere at a heating rate of 10°C/min. All the samples were about 10–11 mg. Samples were first heated to 280°C and held for 5 min to destroy anisotropy; then they were cooled to 30°C and subsequently reheated to 280°C. The melting temperature (T_m) was considered to be the maximum of the endothermic melting peak from the heating scans and the crystallization temperature (T_c) as that of the exothermic peak of crystallization from the cooling scans. The heat of fusion (ΔH_f) and heat of crystallization (ΔH_c) were determined from the areas of the melting peaks and crystallization peaks, respectively, and normalized to the PTT content. All results were the average of three samples.

TGA characterization

The thermal stability of the samples was characterized with a DuPont 910 TG analyzer. The samples were heated under a nitrogen atmosphere at a heating rate of 10°C/min.

RESULTS AND DISCUSSION

Structure of interlayer in organoclay

The WAXD patterns of the clay and organoclay are shown in Figure 1. For these two kinds of clay (8k and 11k), a peak occurs at approximately 2θ = 7.21° (d = 1.23 nm), which corresponds to the basal spacing of the (001) plane of clay. The (001) plane peak of the organoclays (8K-P and 11K-P) is shifted to a lower angle compared to the pristine clays. This indicates that intercalation of the intercalating agent occurred and the interlayer spacing of the clay is increased. A large peak at 2θ = 2.90°, corresponding to 3.04-nm interlayer spacing, is clearly observed for 11K-P. This

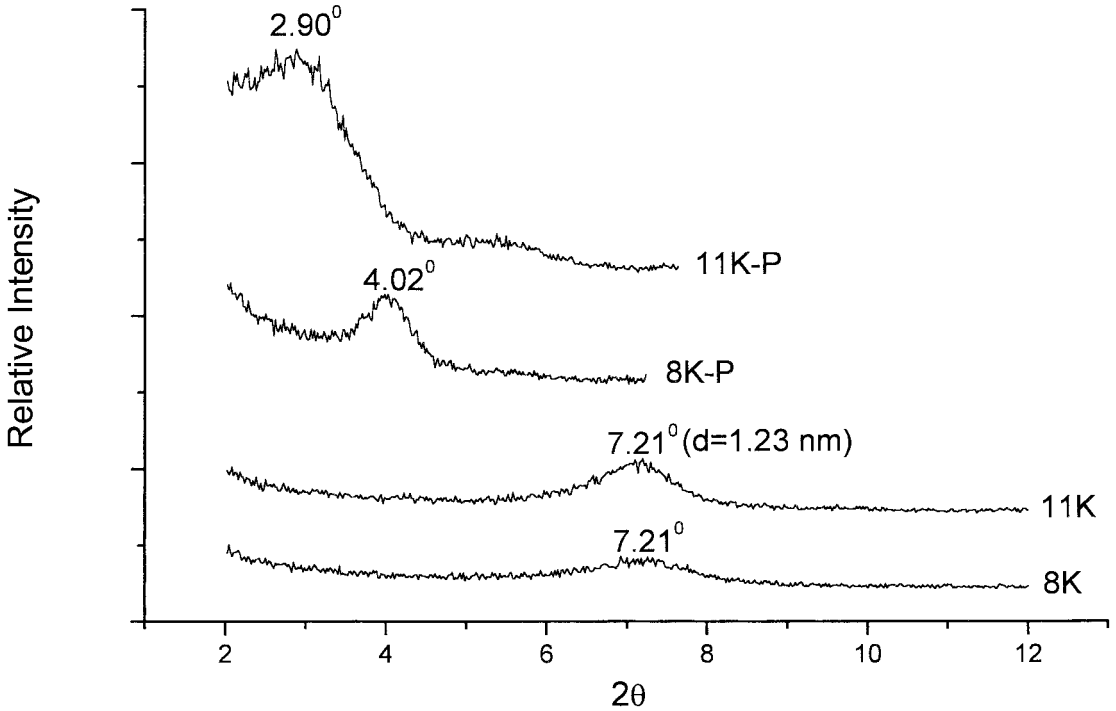

Figure 1 The WAXD patterns of clay and organoclay.

reveals that the interlayer spacing of 11K-P increases from 1.23 to 3.04 nm. The interlayer spacing for 8K-P increases from 1.23 to 2.2 nm (2θ = 4.02°). This fact reveals that the interlayer spacing of organoclay is a function of the CEC of the clay as shown by comparing the WAXD patterns of 11K-P and 8K-P. Organoclay 11K-P exhibits higher interlayer spacing than that of 8K-P. This result indicates that the higher the CEC, the larger the interlayer spacing is. The higher CEC of the clay is conducive to intercalation of the intercalating agent, because the higher CEC of the clay exhibits a higher Na^+ concentration at the same weight.

Dispersibility of organoclay in PTT

The WAXD patterns of organoclay 11K-P and its nanocomposites containing 1, 5, 10, and 15 wt % 11K-P are presented in Figure 2. The (001) plane peaks for the nanocomposites are observed at around 2.7–2.9° and shift to a lower angle compared to 11K-P, except for 1 wt %. The intercalation of the polymer chains usually increases the interlayer spacing, in comparison to the spacing of the organoclay that was used, leading to a shift of the diffraction peak toward lower angle values. In such a nanocomposite, the repetitive multilayer structure is well preserved, allowing the interlayer spacing to be determined. Therefore, it can be concluded that intercalation of PTT chains into the galleries of silicate layers takes place. As previously mentioned, the interlayer spacing of 11K-P is 3.04 nm. At a 95/5 PTT/11K-P ratio, a new and broad peak at 2θ = 2.76° (d = 3.20 nm) was observed and the interlayer spacing increased from 3.04 to 3.20 nm. The WAXD pattern for 90/10 PTT/11K-P is similar to that of 95/5 PTT/11K-P, but it has a small shift to a higher diffraction angle (lower interlayer spacing) compared to 95/5 PTT/11K-P. The interlayer spacing decreases from 3.20 (2θ = 2.76°) to 3.14 nm (2θ = 2.81°) with organoclay loading from 5 to 10 wt %. The WAXD pattern for 85/15 PTT/11K-P is similar to that of organoclay 11K-P, indicating that the interlayer spacing of 85/15 PTT/11K-P is identical to that of organoclay 11K-P. The intercalation of the PTT chain almost did not occur in the 85/15 PTT/11K-P nanocomposite. However, the increase in the interlayer spacing of the organoclay is higher at lower organoclay contents. This result can be explained by the fact that overly large amounts of organoclay cannot be dispersed in PTT and must exist in the form of an agglomerated layer structure. When the clay content is increased to 6 wt %, agglomerated clay particles are observed in poly(ethylene terephthalate-*co*-ethylene naphthalate) (PETN)/organoclay nanocomposites.[19] The intensity and area of WAXD, which peaks at about 2θ = 2.76 and 5.23°, respectively, both increase with an increase in the amount of organoclay loading from 5 to 10 wt %. This indicates that perfect exfoliation of the clay layer structure of the organoclay in PTT does not occur. For these periodic structures, the variation of the interlayer spacing with the weight percentage of organoclay reflects the fact that different polymer/

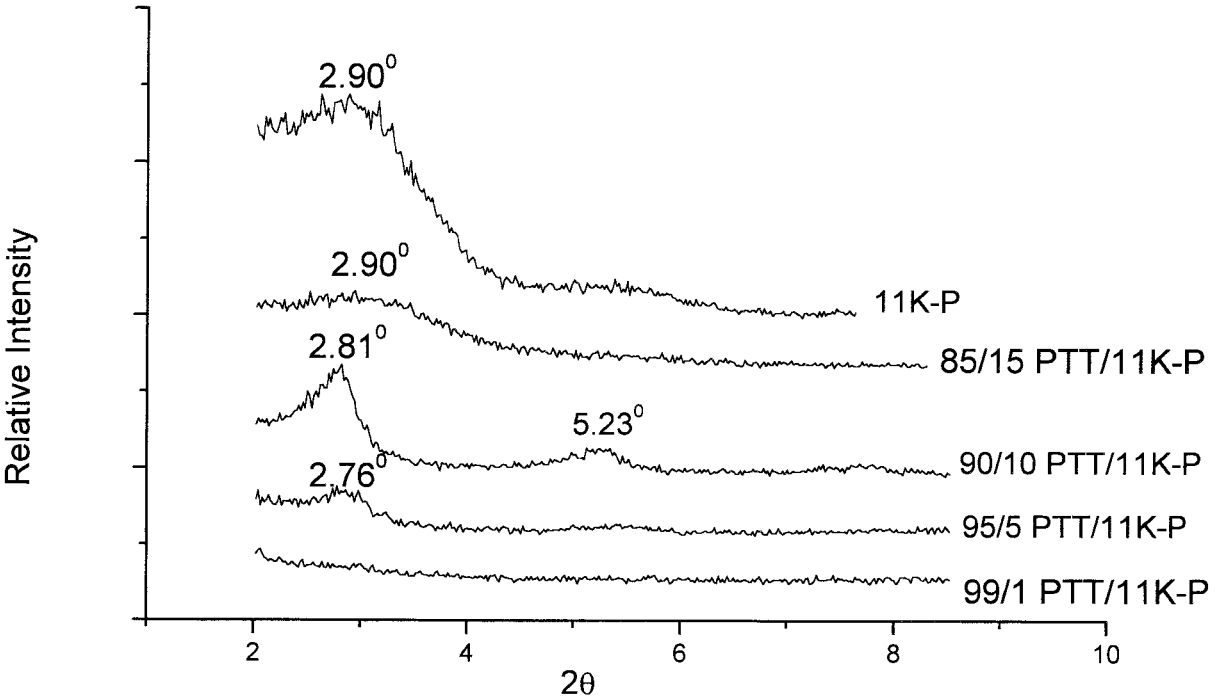

Figure 2 The WAXD patterns of PTT/11K-P nanocomposites.

organoclay weight ratios affect the interlayer spacing of clay.

The nanocomposite containing 1 wt % 11K-P showed no obvious clay peak at around 2.7–2.9° in the WAXD pattern. Thus, at first glance it may be conjectured that most silicate layers lose their crystallographic ordering in the nanocomposite and exfoliation of the organoclay occurs. In addition, it can result from the much lower concentration of organoclay. In the PETN/organoclay nanocomposite,[19] the clay particles may be highly dispersed in the polymer matrix without a large agglomeration of particles for a low clay content (<4 wt %). In this PTT/organoclay nanocomposite, the WAXD patterns for 1 and 5 wt % are similar to those of other PETN/organoclay nanocomposites. The results suggest that both show well-dispersed individual clay layers embedded in the polymer matrix, although a small number of unexfoliated layers still exist.

Effect of organoclay content on crystallization and thermal behaviors of PTT/organoclay nanocomposites

Figure 3 shows cooling and heating curves for PTT/11K-P nanocomposites. The results for the crystallization and thermal parameters are reported in Table I. It is evident that there is a distinct exothermic crystallization peak in all of the cooling scans. The T_c values for the nanocomposites are higher than that of neat PTT (188°C) for all four compositions. Evidently, with the addition of organoclay, the T_c values of the nanocomposites are elevated and 95/5 PTT/11K-P exhibits the highest T_c (197°C). Changes in the crystallization peak width (ΔT_c) and the ΔH_c are related to the overall crystallization rate and the extent of crystallization, respectively. The ΔT_c values for the nanocomposites are narrower by 12–15° than that of neat PTT (30°C), and 99/5 PTT/11K-P exhibits the narrowest ΔT_c (15°C). The crystallization rates are defined as the heat of crystallization divided by the time from the onset to completion of crystallization (ΔH_c/time). As seen in Table I, the values of ΔH_c/time for the nanocomposites are always higher than that of neat PTT (0.291 J/g s). The crystallization rate for 95/5 PTT/11K-P (0.579 J/g s), which is the highest value of ΔH_c/time in all samples, is 1.99 times than that of neat PTT. By increasing the organoclay content to 15%, the value of ΔH_c/time was diminished continuously to the extremely low value of 0.468 J/g s. In other words, the crystallization rates for the PTT/11K-P nanocomposites are always greater than that of PTT and the 95/5 PTT/11K-P exhibits the greatest crystallization rate. These results imply that the crystallization of PTT may be accelerated by means of solution blending with 1–15 wt % of 11K-P and the acceleration effect probably reaches a maximum at a 11K-P level of about 5 wt %. The clay plays a nucleating role to some extent. The results are similar to those for systems of PET/clay,[12] nylon 1212/MMT,[20] and polyamide-6/MMT nanocomposites.[21] In these systems, MMT is an effective nucleating agent.

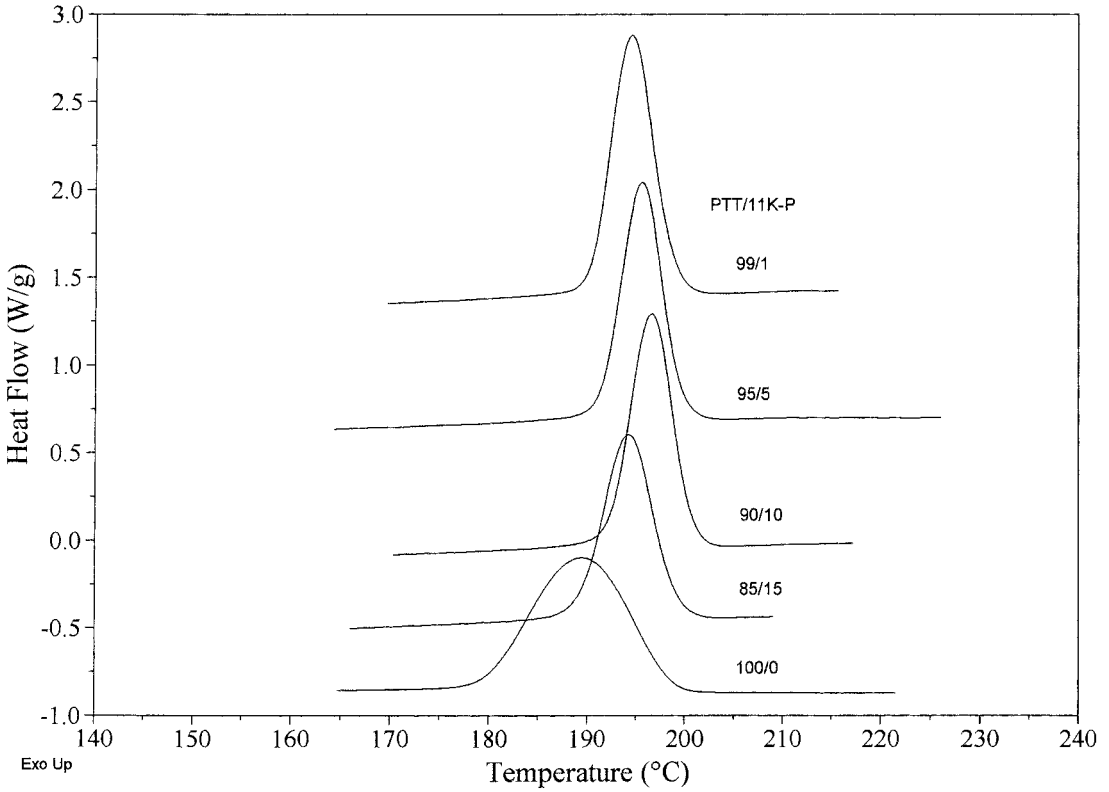

(a)

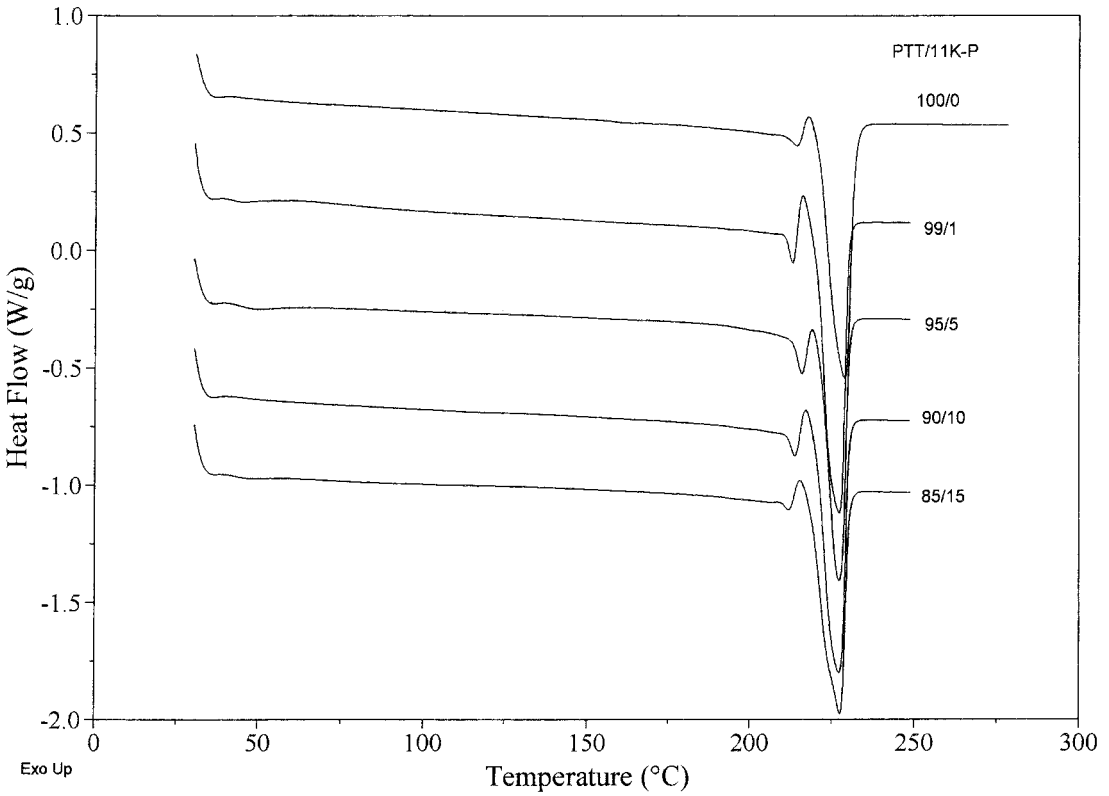

(b)

Figure 3 The DSC thermograms of neat PTT and PTT/11K-P nanocomposites: (a) cooling scans; (b) heating scans.

TABLE I
DSC Data of PTT/11K-P Nanocomposites

PTT/11K-P Composition	Melting (Heating Scans)				Crystallization (Cooling Scans)					
	Onset (°C)	T_m (°C)	ΔT_m (°C)	ΔH_f (J/g)	Onset (°C)	T_c (°C)	ΔT_c (°C)	ΔH_c (J/g)	ΔH_c/time (J/g s)	ΔT[a] (°C)
100/0	214	228	24	48.4	204	188	30	52.4	0.291	40
99/1	216	227	18	55.2	202	194	16	51.5	0.537	33
95/5	217	228	17	53.4	204	197	15	52.1	0.579	31
90/10	217	227	16	52.6	204	196	16	51.0	0.531	31
85/15	216	227	19	53.2	203	194	18	50.7	0.468	33

[a] $\Delta T = T_m - T_c$.

The crystallization temperature reflects the overall crystallization rate in cooling scans because of the combined effects of nucleation and growth. Thus, the degree of supercooling ($\Delta T = T_m - T_c$) may be a measurement of a polymer's crystallizability: the smaller the ΔT, the higher the overall crystallization rate. The ΔT values for the PTT/11K-P nanocomposites are 7–9°C smaller than that of neat PTT (40°C). The results again reveal that the overall crystallization rate for the PTT/11K-P nanocomposites is greater than that of neat PTT.

As shown in Table I, the PTT/ 11K-P nanocomposites exhibit a higher T_c, a greater ΔH_c/time, and a smaller ΔT than those of neat PTT, demonstrating that the clay takes the role of a nucleating agent. The 95/5 PTT/11K-P exhibits the highest T_c (197°C), the greatest ΔH_c/time (0.579 J/g s), the smallest ΔT_c (15°C), and the smallest ΔT (31°C) among the PTT/11K-P nanocomposites. These results imply that the crystallization of PTT may be accelerated by means of blending with 1–15 wt % of 11K-P and the acceleration effect probably reaches a maximum at the 11K-P level of 5 wt %.

There is an endothermic melting peak in all of the heating scans. The various melting parameters determined from heating scans for PTT/11K-P nanocomposites are summarized in Table I. The T_m is virtually unchanged, regardless of organoclay loading. The onset temperatures of melting and the melting peak width (ΔT_m) are related to the least thermal stability and distribution of crystallites, respectively. A small increase (2–3°C) of the onset temperature of melting is found in the nanocomposites compared to that of neat PTT (214°C). A clear decrease (5–8°C) in ΔT_m is found in the nanocomposites with respect to that of neat PTT (24°C). In other words, the distribution of crystallites of PTT in PTT/11K-P nanocomposites is narrower than that of neat PTT. A clear increase in the ΔH_f in the nanocomposites indicates that the crystallinity of PTT in the nanocomposites is higher than that of neat PTT. These results indicate that the perfection of crystallites of PTT in the nanocomposites is not destroyed by 1–15 wt % of 11K-P.

Thermal stability

Figure 4 shows the TGA curves of PTT/11K-P nanocomposites with different 11K-P content. The thermal decomposition temperatures (T_d, from the differential TG traces, not shown) and the weight percentage of residue at 600°C are listed in Table II. It is observed that most of the nanocomposites possess slightly higher thermal stability than neat PTT, except for 85/15 PTT/11K-P. The T_d of neat PTT is 399°C. Those of the nanocomposites have a small increase with increases of up to 10 wt % organoclay, and 99/1 PTT/11K-P exhibits the highest T_d (403°C). When increasing the organoclay content to 15%, the T_d was diminished to an extremely low value of 398°C. The increase in the thermal stability of the nanocomposites may result from the barrier effect of the clay layer structure and from the strong interaction between the organoclay and PTT molecules.[22] Furthermore, the clay platelets have a shielding effect on the matrix and slow the rate of mass loss of the decomposition product. For PETN/MMT nanocomposites,[19] a similar trend for the thermal stability with increasing MMT (<6 wt %) was observed. In the MMT/polyimide hybrids,[23] the hybrids possessed higher thermal stability when the MMT (<10 wt %) was well dispersed. As the MMT content increases, the agglomeration tendency of MMT increases and the thermal stability decreases. The thermal stability of PET/clay nanocomposites showed a 6–19°C increase with 1.5–5.0 wt % organoclay.[12] Ke et al.[12] explains that the nanoscale particles will show a stronger interaction with the matrices of PET when the external temperature approaches the degradation temperature. The molecular structure of PTT is similar to that of PET. We believe that the enhancement of the thermal stability of PTT by 1–10 wt % organoclay resulted from the same cause as the PET/clay nanocomposites.[12] When the clay loading increases to 15 wt %, the excessive amount of clay (>10 wt %) decreases the thermal stability of PTT/ 11K-P nanocomposites. This suggests that the organoclay 11K-P domain can agglomerate above 10 wt % 11K-P content in the PTT matrix. As seen in Table II,

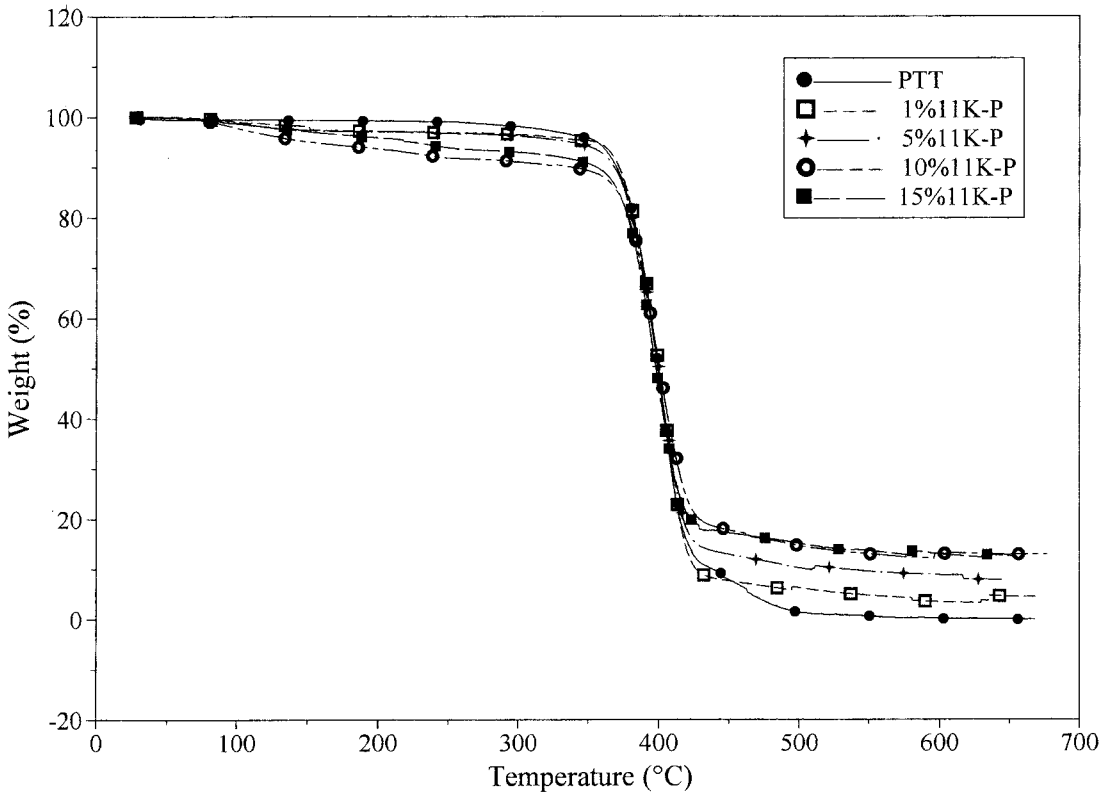

Figure 4 The TGA curves of PTT/11K-P nanocomposites.

the weight of the residue at 600°C increases, ranging from 3.5 to 12.3 wt % with organoclay loadings of 1–15 wt %. This enhancement of char formation is ascribed to the high heat resistance exerted by the MMT itself.[24]

In this research, thermal stability was enhanced at low organoclay content because of the difference in the chemical structure and the restricted thermal motion of the PTT in the silicate interlayer. Optimal thermal stabilization is obtained at a clay content of about 1–5 wt %. Too much clay (>10 wt %) decreases the thermal stability of PTT/11K-P nanocomposites because of the agglomeration of clay. The results reveal that the thermal stability of PTT/11K-P nanocomposites is related to the organoclay 11K-P content and the dispersion of 11K-P in the PTT matrix.

TABLE II
TGA Data of PTT/11K-P Nanocomposites

PTT/11K-P Composition	T_d (°C)	wt_R^{600} (%)
100/0	399	0.3
99/1	403	3.5
95/5	401	8.1
90/10	402	11.8
85/15	398	12.3

T_d, The temperature at the maximum weight loss rate; wt_R^{600}, weight percentage of residue at 600°C.

CONCLUSIONS

We prepared PTT/11K-P nanocomposites by solution blending. Our WAXD analysis indicated that intercalated nanocomposites were obtained.

The results of the DSC analysis demonstrate that clay is an effective nucleating agent and it increases the crystallization rate of PTT/11K-P nanocomposites. The thermal stability of the nanocomposite with organoclay 11K-P loading from 1 to 10 wt % is higher than that of neat PTT.

The author would like to thank the National Science Council of the Republic of China for financially supporting this research (NSC 90-2216-E-167-002).

References

1. Ellsworth, M. W.; Gin, D. L. Polym News 1999, 24, 331.
2. Calvert, P. D. Mater Res Soc Bull 1992, 17, 37.
3. Giannelis, E. P. Adv Mater 1996, 8, 29.
4. Komarneni, S. J. Mater Chem 1992, 2, 1219.
5. Usuki, A.; Kojima, Y.; Kawasumi, M.; Okada, A.; Fukushima, Y.; Kurauchi, T.; Kamigaito, O. J Mater Res 1993, 8, 1179.
6. Yano, K.; Usuki, A.; Kurauchi, T.; Kamigaito, O. J Polym Sci Part A Polym Chem 1993, 31, 2493.
7. Messersmith, P. B.; Giannelis, E. P. Chem Mater 1994, 6, 1719.
8. Messersmith, P. B.; Giannelis, E. P. J Polym Sci Part A Polym Chem 1995, 33, 1047.

9. Burnside, S. D.; Giannelis, E. P. Chem Mater 1995, 7, 1597.
10. Vaia, R. A.; Vasudevan, S.; Krawiec, W.; Scanlon, L. G.; Giannelis, E. P. Adv Mater 1995, 7, 154.
11. Gilman, J. W.; Morgan, A. B.; Harris, R. H.; Trulove, P. C.; Delong, H. C.; Sutto, T. E. Polym Mater Sci Eng 2000, 83, 59.
12. Ke, Y.; Long, C.; Qi, Z. J Appl Polym Sci 1999, 71, 1139.
13. Maxfield, M.; Shacklette, L. W.; Baughman, R. H.; Christiani, B. R.; Eberly, D. E. Int. Pat. WO 93/04118, 1993.
14. Di Lorenzo, M. L.; Raimo, E.; Cascone, E.; Martuscelli. J Macromol Sci Phys 2001, B40(5), 639.
15. Traub, H. L. Angew Makromol Chem 1995, 179, 4055.
16. Poulin-Dandurand, S.; P'erez, S.; Revol, J. F.; Brisse, F. Polymer 1979, 20, 419.
17. Desborough, I. J.; Hall, I. H.; Neisser, J. Z. Polymer 1979, 20, 545.
18. Pyda, M.; Boller, A.; Grebowicz, J.; Chuah, H.; Lebedev, B. V.; Wunderlich, B. J Polym Sci Part B Polym Phys 1998, 36, 2499.
19. Cheng, J. H.; Park, D. K. J Polym Sci Part B Polym Phys 2001, 39, 2581.
20. Wu, Z.; Zhou, C.; Zhu, N. Polym Test 2002, 21, 479.
21. Akkapeddi, M. K. Polym Compos 2000, 21, 576.
22. Petrovic, X. S.; Javni, I.; Waddong, A.; Banhegyi, G. J Appl Polym Sci 1999, 3, 2063.
23. Yang, Y.; Zhu, Z. K.; Yin, J.; Wang, X. Y.; Qi, Z. E. Polymer 1999, 40, 4407.
24. Frischer, H. R.; Gielgens, L. H.; Koster, T. P. M. Acta Polym 1999, 50, 122.